Analysis of Highly Sensitive Photonic Crystal Biosensor for Glucose Monitoring

M. S. Mohamed [1], Mohamed Farhat O. Hameed [2,3], Nihal F. F. Areed [2,4], M. M. El-Okr [5], and S. S. A. Obayya [2]

[1] Basic Science Department, Faculty of Engineering
Misr University for Science and Technology (MUST), El-Motamyez Uptown, 6th of October City, Giza, Egypt

[2] Centre for Photonics and Smart Materials, Zewail City of Science and Technology
Sheikh Zayed District, 6th of October City, Giza, Egypt
sobayya@zewailcity.edu.eg

[3] Mathematics and Engineering Physics Department, Faculty of Engineering
Mansoura University, Mansoura 35516, Egypt

[4] Department of Electronics and Communications Engineering, Faculty of Engineering
Mansoura University, Mansoura 35516, Egypt

[5] Physics Department, Faculty of Science
Al-Azhar University, Nasr City, Cairo, Egypt

Abstract ─ In this study, a novel compact and fully integrated 2D photonic crystal (PhC) biosensor with high sensitivity has been proposed for Glucose monitoring. The simulation results are obtained using 2D finite element time domain method (FETDM). To evaluate the performance of the suggested design, the transmission spectrum through the reported structure has been calculated. The effect of the structure geometrical parameters of the biosensor is studied to maximize the biosensor sensitivity. The suggested biosensor offers high sensitivity of 422 nm/RIU with high linearity. Additionally, the suggested biosensor has a simple design and is easy for fabrication. The enhancement of the sensitivity of the PhC biosensor is very important to amplify the detection of the small variation in analyte's physical properties. Therefore, the achieved sensitivity enhancement can improve the applications of Glucose monitoring.

Index Terms ─ Biosensor, finite element time domain method, photonic crystal, sensitivity, transmission.

I. INTRODUCTION

Biosensors are devices used for detecting and analyzing samples with different characteristics [1,2]. The work in the biosensors depends on the response to the change in the physical properties of the analyzed samples. There are a lot of types of biosensors such as physicochemical, piezoelectric, optical, and electro-chemical biosensors. The sensing in the biosensors represents the detecting power against the change in the physical properties of the analyzed samples. The biosensors have a wide range of applications such as food analysis, DNA classifications, microbial biosensors, and Glucose monitoring [3]. Therefore, biosensors have attracted the interest of many researchers all over the world. Recently, the photonic crystal (PhC) biosensor has gained enormous interest due to its simplicity and high sensitivity [4-8]. The 2D PhCs have many related applications such as waveguides, logic gates [9], filters [10], polarization converters [11], PhC router and PhC image encryptors [12,13]. Additionally, the 2D PhC can confine the optical state in very small dimensions. Making a defect through the periodicity of the structure of a 2D PhC shows allowed modes in the photonic bandgap region [14]. The transmission of the electromagnetic wave through the defected area is affected by the change of refractive indices of the composed material. For these reasons, the 2D PhC is exploited for biosensing applications. The sensitivity of the 2D PhC biosensor can be calculated by measuring the shift in resonance wavelength at which maximum transmission through PhC structure occurs. The more displacement of peaks with a satisfied quality factor, the higher sensitivity that can be obtained [4,5]. In this regard, Hsiao and Lee [4] have reported a computational study of PhC nano-ring resonator for biochemical sensing with a maximum sensitivity of 6 nm/RIU. Additionally, Pal et

al. [15] have achieved a sensitivity of 64.5 nm/RIU using hetero-structure slab PhC by detecting the resonance wavelength for analytes of air, water, and isopropanol. Further, Olyaee et al. [5] have investigated four-channel label-free PhC biosensor using nanocavity resonators which offer a sensitivity of 65.7 nm/RIU. Moreover, Dorfner et al. [16] have enhanced the sensitivity to 103±1 nm/RIU using different concentrations of bovine serum albumin (BSA) solution. Further, Kim et al. [17] reported a sensitivity of 135 nm/RIU by using matched liquids at different five refractive indices from 1.296 to 1.372 with a step of 0.019. Further, Najafgholinezhad and Olyaee [6] have presented PhC biosensor with the temperature dependent investigation of microcavity resonator with a sensitivity of 141.67 nm/RIU. Dündar et al. [18] have also studied different concentrations of sugar-water solutions which resulted in a sensitivity of 280 nm/RIU. In addition, Kita et al. [19] have used liquids of refractive indices from 1.00 to 1.37, and they have demonstrated a sensitivity of 350 nm/RIU. In this paper, a novel design of 2D PhC biosensor with high sensitivity is proposed and analyzed. The effect of the structure geometrical parameters of the reported design on the biosensor sensitivity is investigated to maximize the biosensor sensitivity. In this regard, the effect of the radius of the central microcavity in the midway of the defected 2D PhC is studied thoroughly. Additionally, the impact of the surrounding holes around the central microcavity that are filled with the glucose solution is reported. The simulation results are obtained by using finite element time domain method (FETDM) [20-22]. The suggested biosensor offers high sensitivity of 422 nm/RIU which is greater than that reported in [4-6, 15-19]. Further, the proposed biosensor has an easy and accurate label-free performance due to the detection of the target molecules in their natural form. The molecular interaction due to the change in the glucose concentration results in an analyte refractive index variation. Consequently, resonance wavelength shift will occur and hence the biosensor sensitivity can be obtained. In this study, the sensitivity is defined as the resonance wavelength shift $\Delta\lambda$ per analyte refractive index change Δn [5]. The detection of the resonance wavelength shift gives information about the corresponding glucose concentration change and the corresponding molecular interactions. Moreover, the suggested label-free PhC biosensors can effectively measure the effective refractive index variation near the active sensing surface.

II. PHOTONIC BANDGAP STRUCTURE

The considered PhC platform consists of GaN dielectric slab drilled with air holes. The air holes of radius r = 0.345a are forming hexagonal lattice as shown in Fig. 1 (a) with a lattice constant a = 500 nm. The dielectric constant of the GaN dielectric slab is equal to 4.94 at wavelength λ = 1400 nm.
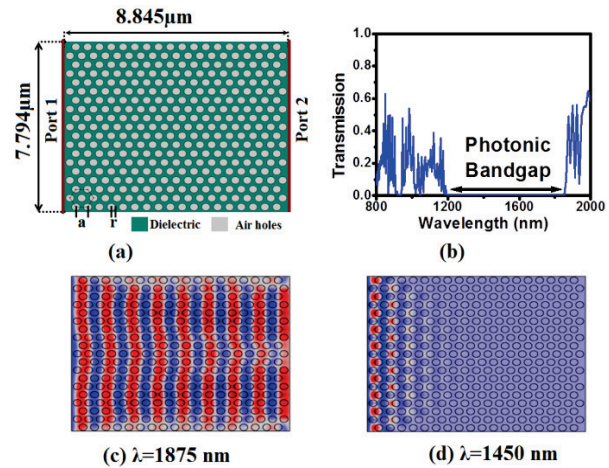

Fig. 1. (a) Cross-section of 2D PhC, (b) transmission spectrum curve through the 2D PhC, (c) field distribution at λ = 1875 nm, and (d) field distribution at λ = 1450 nm.

The GaN has a wide range of applications in different optical fields such as light emitting diodes (LEDs) and solar cells [23, 24]. It has very high crystalline quality due to its low-temperature depositing [25]. Further, the GaN is insoluble in water [26]. Additionally, the GaN can be operated in different applications under high temperature like optoelectronics (charge screening, light flow control) [27,28]. The GaN is also a good candidate for photonic crystal applications [29] due to the high index contrast between its dielectric permittivity of 4.94 and that of the air. Therefore, a good confinement can be obtained through the defected channel with the analyte filled central cavity and hence high sensitivity can be obtained. The transmission value T is calculated from the formula $T = |E_{out}/E_{in}|^2$, where E_{in} is the incident input field by port 1 and E_{out} is the received output field by port 2. Figure 1 (b) represents the transmission spectra through the 2D PhC. It evident from this figure that there is a photonic bandgap from λ = 1200 nm to 1850 nm. Figures 1 (c) and 1 (d) present the field distributions at wavelengths of 1875 nm and 1450 nm, respectively. The field distribution diagrams are in consistence with the transmission shown in Fig. 2 (b). At λ=1875 nm, the light is propagating through the PhC structure while it is forbidden at a wavelength of 1450 nm. The photonic bandgap range is necessary for selecting the allowed modes for the suggested 2D PhC biosensor. The effects of the structure geometrical parameters on the sensitivity of the proposed designs have been studied using the FETDM with perfectly matched layer boundary conditions [21, 22]. In this study, the size of the finite elements variates from 0.00285 to 0.637 μm. The element growth rate that determines how fast the elements should grow from small to large over the studied domain is equal to 1.3. Additionally, the curvature factor that limits how large the element size

can be along the curved boundaries of the suggested structure is fixed at 0.3.

III. DESIGN CONSIDERATION AND NUMERICAL RESULTS

As shown in Fig. 2 (a), the 2D PhC biosensor is formed by removing the central horizontal row of air holes from the basic composition of the studied 2D PhC. Further, a microcavity of radius R is added in the midway of the central channel defect. The central cavity is filled with analyte sample of glucose solution with refractive index [30]:

$$n=0.00011889C+1.33230545, \qquad (1)$$

where C is the glucose concentration in (g/L). The effect of the microcavity radius R on the sensitivity is studied to maximize the biosensor sensitivity. In this study, Gaussian pulse of width 0.4 µm with a central carrier wavelength of 1.4 µm has been adopted to feed the proposed structure from port 1. The change in the concentration of the glucose affects the transmission of the traveling electromagnetic wave as shown in Fig. 2.
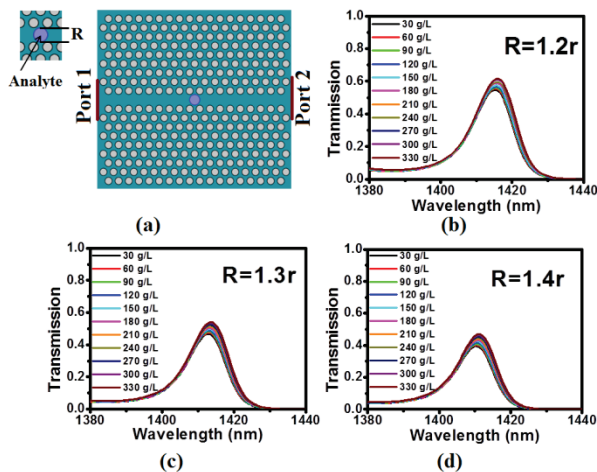

Fig. 2. (a) The cross-section of the 2D PhC biosensor with the central microcavity filled with the analyte (glucose solution). The transmission spectra through the proposed 2D PhC biosensor with microcavity of radii: (b) R=1.2r, (c) R=1.3r, and (d) R=1.4r.

Figures 2 (b), 2 (c), and 2 (d) show the transmission spectra that are obtained at different radii of the microcavity, 1.2r, 1.3r, and 1.4r at different glucose concentrations. It is revealed from these figures that the displacement of the peaks due to changes in the analyte refractive index is weak. Therefore, very small sensitivity can be obtained for the suggested design. Figure 3 shows the variation of the resonance wavelength with the glucose concentration at different R values. It is evident from this figure that the resonance wavelength is slightly affected by the change in the glucose concentrations.

Therefore, the sensitivity of the proposed sensor will be very small. In this study, the sensitivity is defined as the resonance wavelength shift per the change in the analyte refractive index ($\Delta\lambda/\Delta n$) [5]. The Δn change is calculated according to the change in the glucose concentration as may be noted from Equation (1). In order to enhance the transmission and the sensitivity of the 2D PhC biosensor, the radius of the central microcavity is increased and some of the surrounding air holes are removed.
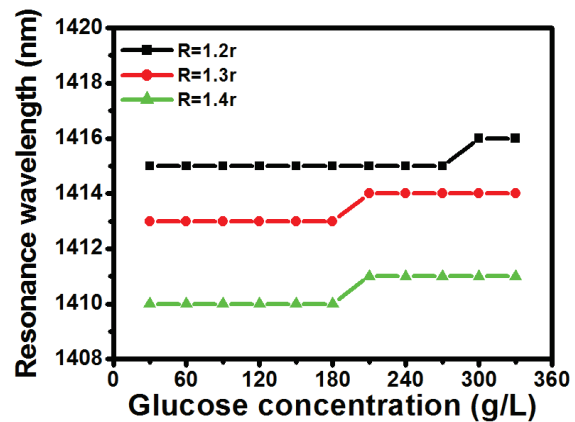

Fig. 3. The shift in the resonance wavelength as a function of the glucose concentration at different R values 1.2r, 1.3r, and 1.4r.

The new design of the 2D PhC biosensor is shown in Fig. 4 (a). Figure 4 (b) and 4 (c) show the field distribution at R=3.4r and 1.4r at the corresponding resonance wavelengths 1403 nm and 1411 nm, respectively at concentration c=330 g/L. It is revealed from these figures that the transmission through the PhC design is enhanced by increasing the central cavity radius R from 1.2r to 3.4r. Figures 5 (a), 5 (b), and 5 (c) show the transmission through the suggested sensor at different glucose concentrations and at different microcavity radii R. It is evident from these figures that the sensitivity and transmission increase by using the improved design. At R = 3r, 3.2r and 3.4r, the sensitivity is equal to 35 nm/RIU, 201.4 nm/RIU, and 186.5 nm/RIU, respectively. All of these results are also confirmed in Fig. 5 (d), where the resonant wavelengths are plotted against the glucose concentration change. Due to the index contrast between the refractive indices of the GaN and the glucose solution, reflection and refraction occur to the introduced electromagnetic beam in the proposed structure. The measured transmission depends on the refraction when the electromagnetic wave transfers from the GaN to the glucose solution [31]. As the microcavity radius increases, the amount of filled glucose solution and its effect on the transmission of the traveling electromagnetic wave through the defected region will be increased. Consequently, the shift in the resonance

wavelength due to the glucose refractive index change can be detected with high sensitivity.
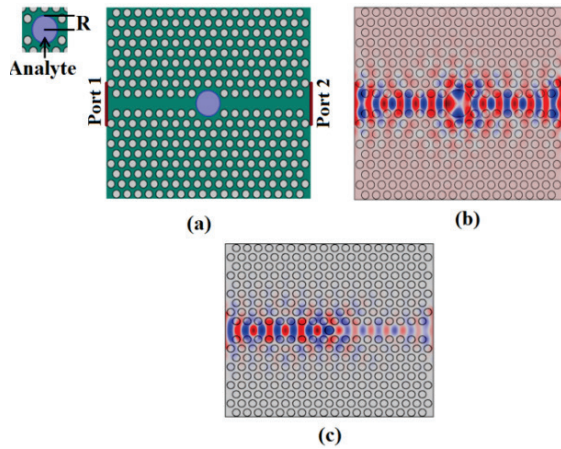

Fig. 4. (a) Cross-section of the 2D PhC biosensor with the large central microcavity filled with the analyte (glucose solution). Field distribution through the suggested design with glucose concentration c=330 g/L at: (b) R=3.4r (λ=1403 nm) and (c) R=1.4r (λ=1411 nm).
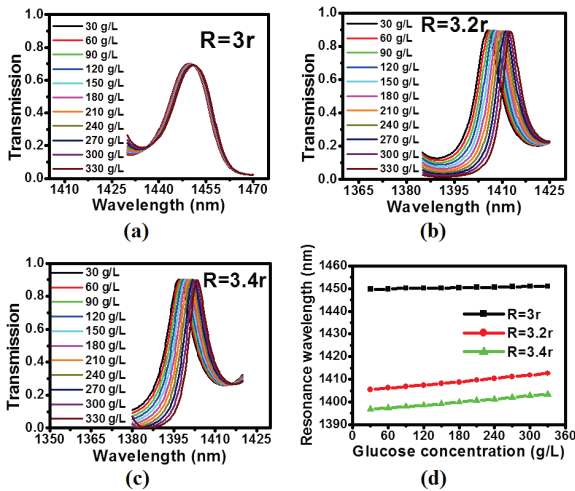

Fig. 5. The transmission spectra through the proposed biosensor at different glucose concentrations at: (a) R = 3r, (b) R = 3.2r, (c) R = 3.4r, and (d) shift in the resonance wavelength as a function of the glucose concentration at different microcavity radii.

In order to further increase the sensitivity and transmission of the proposed sensor, the surrounding holes around the central microcavity are filled with the glucose solution as shown in Fig. 6 (a). Additionally, it is important from the practical point of view to keep the minimum separation between the edges of the central microcavity and the surrounding holes filled by glucose solution at 15 nm. This separation value is the suitable

limit in the practical consideration. Then, the radius of the central microcavity R is tested with values of 3r, 3.1r, and 3.2r as shown in Figs. 6 (b), 6 (c), and 6 (d). It is observed from these figures that the shift in the resonance wavelength becomes greater than that in the previous tests. It is also noted that the sensitivity increases with increasing the radius of the central microcavity in this structure. The shift in the resonance wavelengths as a function of the glucose concentration is represented in Fig. 7. It is evident from this figure that the resonance wavelength changes linearly with the glucose concentration change. The biosensor sensitivities are equal to 280 nm/RIU, 301.3 nm/RIU and 330.3 nm/RIU corresponding to R=3r, 3.1r, and 3.2r, respectively.
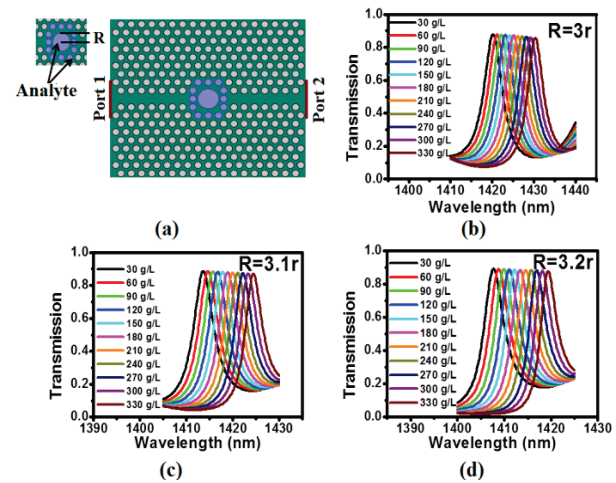

Fig. 6. (a) Cross-section of the modified 2D PhC biosensor with large central microcavity surrounded by 12 holes filled with the analyte (glucose solution). The transmission spectra at different glucose concentrations at: (b) R = 3r, (c) R = 3.1r, and (d) R = 3.2r.
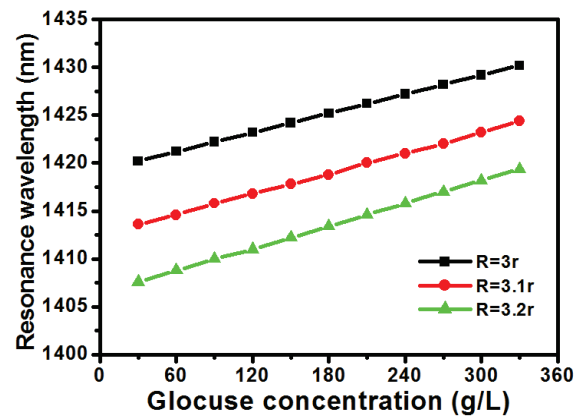

Fig. 7. The shift in the resonance wavelength as a function of the glucose concentration for the suggested 2D PhC biosensor at different R values.

In order to enhance the sensitivity of the suggested 2D PhC biosensor, the ellipticity of the central microcavity surrounded by holes filled with glucose solution is studied. In this investigation, the effect of the major diameter is changed from 2.2a to 2.6a with a step of 0.1a. However, the minor diameter is fixed at 2.2a because of practical consideration to keep the minimum separation between the edges of surrounding holes filled with glucose solution and the central microcavity at 15 nm. It is evident from Fig. 8 that the sensitivity is affected by changing the major diameter of the elliptical microcavity. The proposed 2D PhC biosensor offers high sensitivity of 422 nm/RIU at the major radius 2.6a which is greater than that reported in [16-19].
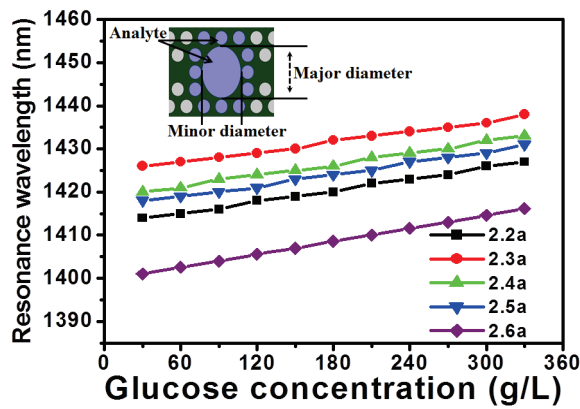

Fig. 8. Shift in the resonance wavelength as a function of glucose concentration at different values of the major diameter of the elliptical microcavity.

The quality factor of the suggested biosensor is also evaluated using the resonance wavelength λ_o and the full width at the half maximum of the output transmission $\Delta\lambda_{FWHM}$ as given by $(\lambda_o/\Delta\lambda_{FWHM})$. The numerical results reveal that the suggested PhC biosensor has an average quality factor of 549.2. The crosstalk (CT) of the proposed 2D PhC biosensor is calculated as [13]:

$$CT = 20 \log (T_{desired} / T_{undesired}), \qquad (2)$$

where $T_{desired}$ is the desired transmission at certain resonance wavelength and $T_{undesired}$ is the undesired transmission at the same resonance wavelength. The proposed 2D PhC offers an average CT of 20 dB which shows the effectiveness of the proposed biosensor.

IV. EXPERIMENTAL APPROACH

In this study, the GaN dielectric slab is used as a background material for the suggested PhC biosensor. There are different techniques that are used to grow the GaN dielectric slab [32-35].The nitride-based layers can be grown on silicon substrates by selective wet etching. The selective wet etching process starts with the growth of multilayer structure by metal organic vapor epitaxy on Si (111) substrate. Then, the drilled air holes of the

photonic crystal structure are formed by inductively coupled plasma etching process [32-34]. The GaN dielectric slab can also be produced by selective thermal decomposition (STD) technique. In this regard, the GaN is selectively decomposed at a temperature of ~1000ºC under NH_3/H_2 ambient conditions and the drilled air holes are formed by using electron beam lithography method (EBLM). Arita et al. (2012) have used the STD and high crystalline nitride dielectric slab with the highly smoothed surface has been obtained [35]. Additionally, Baroni et al. (2010) have demonstrated tunable cavities with different sizes filled with liquid crystals (LCs). They have used free standing Si using a membrane to ease the infiltration of LC into the holes in the photonic structure. A glue can also be used to block the unfilled air holes. Therefore, it is believed that the suggested design with the selectively filled central cavity and surrounding air holes can be achieved successfully [36]. Further, the elliptical microcavity hole could be established practically as reported by Quiñónez et al. [37] and Vogelaar et al. [38].

V. CONCLUSION

A novel, compact and highly sensitive biosensor based on PhC platform has been proposed and analyzed in this paper. The 2D PhC biosensor comprises a hexagonal lattice of cylindrical holes that are perforated in a dielectric material. A gradation in the change of the 2D PhC biosensor structure tends to enhance the sensitivity. It is found that the 2D PhC biosensor with elliptical microcavity surrounded by holes filled with analyte exhibits the highest sensitivity of 422 nm/RIU. The numerical results also reveal that the wavelength shift is linearly proportional to the glucose concentration. Further, the proposed design has an amplified sensitivity with high detection of small variation in the glucose concentration. The enhancement of the 2D PhC biosensor will give high quality promising applications for glucose monitoring.

REFERENCES

[1]   A. P. F. Turner, I. Karube, and G. S. Wilson, *Biosensors Fundamentals, and Applications*. Oxford University Press, 1987.

[2]   F. G. Bănică, *Chemical Sensors, and Biosensors: Fundamentals and Applications*. John Wiley & Sons, 2012.

[3]   A. Cavalcanti, B. Shirinzadeh, M. Zhang, and L. C. Retly, "Nanorobot hardware architecture for medical defense," *Sensors*, vol. 8, no. 5, pp. 2932-2958, May 2008.

[4]   F. Hsiao and C. Lee, "Computational study of photonic crystals nano-ring resonator for biochemical sensing," *IEEE. Sens. J.*, vol. 10, no. 7, pp. 1185-1191, July 2010.

[5]   S. Olyaee, S. Najafgholinezhad, and H. A. Banaei,

"Four-channel label-free photonic crystal biosensor using nanocavity resonators," *Photonic Sensors*, vol. 3, no. 3, pp. 231-236, September 2013.

[6] S. Najafgholinezhad and S. Olyaee, "A photonic crystal biosensor with temperature dependency investigation of micro-cavity resonator," *Optik*, vol. 125, pp. 6562-6565, November 2014.

[7] S. I. Azzam, Mohamed F. O. Hameed, R. E. A. Shehata, A. M. Heikal, and S. S. A. Obayya, "Multichannel photonic crystal fiber surface plasmon resonance based sensor," *Journal of Optical Quantum Electronics*, vol. 48, no. 142, pp. 1-11, February 2016.

[8] M. F. O. Hameed, M. El-Azab, A. M. Heikal, S. M. El-Hefnawy, and S. S. A. Obayya, "Highly sensitive plasmonic photonic crystal temperature sensor filled with liquid crystal," *IEEE Photonics Technology Letter*, vol. 28, no. 1, pp. 59-62, October 2015.

[9] R. M. Younis, N. F. F. Areed, and S. S. A. Obayya, "Fully integrated AND and OR optical logic gates," *IEEE Photonics Technology Letters*, vol. 26, no. 19, pp. 1900-1903, October 2014.

[10] M. F. O. Hameed, A. M. Heikal, B. M. Younis, M. Abdelrazzak, and S. S. A. Obayya, "Ultra-high tunable liquid crystal-plasmonic photonic crystal fiber polarization filter," *Journal of Optics Express*, vol. 23, no. 6, pp. 7007-7020, March 2015.

[11] M. F. O. Hameed, M. Abdelrazzak, and S. S. A. Obayya, "Novel design of ultra-compact triangular lattice silica photonic crystal polarization converter," *IEEE J. Lightwave Technology*, vol. 31, no. 1, pp. 81-86, January 2013.

[12] N. F. F. Areed and S. S. A. Obayya, "Novel design of symmetric photonic bandgap based image encryption system," *Prog. Electromagn. Res. C*, vol. 30, pp. 225-239, June 2012.

[13] N. F. F. Areed and S. S. A. Obayya, "Novel all-optical liquid photonic crystal router," *IEEE Photonic Tech. L.*, vol. 25, no. 13, pp. 1254-1256, May 2013.

[14] J. D. Joannopoulos, S. G. Johnson, J. N. Winn, and R. D. Meade, *Photonic Crystals Molding the Flow of Light*. Princeton University Press, 2007.

[15] S. Pal, E. Guillermain, R. Sriram, B. L. Miller, and P. M. Fauchet, "Silicon photonic crystal nanocavity-coupled waveguides for error-corrected optical biosensing," *Biosens. Bioelectron.*, vol. 26, pp. 4024-4031, June 2011.

[16] D. Dorfner, T. Zabel, T. Hürlimann, N. Hauka, L. Frandsen, U. Rant, G. Abstreiter, and J. Finley, "Photonic crystal nanostructures for optical biosensing applications," *Biosens. Bioelectron.*, vol. 24, pp. 3688-3692, May 2009.

[17] S. Kim, J. Lee, H. Jeon, and H. J. Kim, "Fiber-coupled surface-emitting photonic crystal band edge laser for biochemical sensor applications," *Appl. Phys. Lett.*, vol. 94, 133503, April 2009.

[18] M. A. Dündar, E. C. I. Ryckebosch, R. Nötzel, F. Karouta, L. J. Van Ijzendoorn, and R. W. Van der Heijden, "Sensitivities of InGaAsP photonic crystal membrane nanocavities to hole refractive index," *Opt. Express*, vol. 18, no. 5, pp. 4049-4056, March 2010.

[19] S. Kita, K. Nozaki, and T. Baba, "Refractive index sensing utilizing a CW photonic crystal nanolaser and its array configuration," *Opt. Express*, vol. 16, no. 11, pp. 8174-8180, May 2008.

[20] H. Butt, Q. Dai, and T. D. Wilkinson, "Photonic crystals & metamaterial filters based on 2D arrays of silicon nanopillars," *Prog. Electromagn. Res.*, vol. 113, pp. 181-183, February 2011.

[21] P. Seshu, *Text Book of Finite Element Analysis*. PHI, 2012.

[22] S. Obayya, *Computational Photonics*. John Wiley & Sons, 2011.

[23] H. Amano, M. Kito, K. Hiramatsu, and I. Akasaki, "P-Type conduction in Mg-doped GaN treated with low-energy electron beam irradiation (LEEBI)," *Japanese Journal of Applied Physics*, vol. 28, L2112, December 1989.

[24] Y. Arakawa, "Progress in GaN-based quantum dots for optoelectronics applications," *IEEE Journal of Selected Topics in Quantum Electronics*, vol. 8, no. 4, pp. 823-832, August 2002.

[25] H. Amano, N. Sawaki, I. Akasaki, and Y. Toyoda, "Metalorganic vapor phase epitaxial growth of a high quality GaN film using an AlN buffer layer," *Applied Physics Letters*, vol. 48, no. 5, pp. 353, 1986.

[26] C. M. Foster, R. Collazo, Z. Sitar, and A. Ivanisevic, "Aqueous stability of Ga- and N-polar gallium nitride," *Langmuir*, vol. 29, pp. 216-220, 2013.

[27] A. Di Carlo, "Tuning optical properties of GaN-based nanostructures by charge screening," *Physica Status Solidi*, (a), 183, pp. 81-85, January 2001.

[28] S. J. Pearton, C. R. Abernathy, M. E. Overberg, G. T. Thaler, A. H. Onstine, B. P. Gila, F. Ren, B. Lou, and J. Kim, "New applications advisable for gallium nitride," *Materials Today*, vol. 5, no. 6, pp. 24-31, June 2002.

[29] X. X. Fu, B. Zhang, X. Kang, J. Deng, C. Xiong, T. Dai, X. Jiang, T. Yu, Z. Chen, and G. Zhang, "GaN-based light-emitting diodes with photonic crystals structures fabricated by porous anodic alumina template," *Opt. Exp.*, 19(s5), pp. 1104-1108, 2011.

[30] Y. L. Yeh, "Real-time measurement of glucose concentration and average refractive index using a laser interferometer," *Opt. Lasers Eng.*, vol. 46, pp. 666-670, September 2008.

[31] H. Sato, H. Iba, T. Naganuma, and Y. Kagawa, "Effects of the difference between the refractive indices of constituent materials on the light transmittance of glass-particle-dispersed epoxy-matrix optical composites," *Philosophical Magazine B*, vol. 82, no. 13, pp. 1369-1386, 2002.

[32] D. Néel, S. Sergent, M. Mexis, D. Sam-Giao, T. Guillet, C. Brimont, T. Bretagnon, F. Semond, B. Gayral, S. David, X. Checoury, and P. Boucaud, "AlN photonic crystal nanocavities realized by epitaxial conformal growth on nanopatterned silicon substrate," *Appl. Phys. Lett.*, vol. 98, 261106, June 2011.

[33] N. V. Triviño, G. Rossbach, U. Dharanipathy, J. Levrat, J. A. Castiglia, J. F. Carlin, K. A. Atlasov, R. Butté, R. Houdré, and N. Grandjean, "High-quality factor two dimensional GaN photonic crystal cavity membranes grown on silicon substrate," *Appl. Phys. Lett.*, vol. 100, 071103, February 2012.

[34] T. T. Wu, S. Y. Lo, H. M. Huang, C. T. Tsao, T. C. Lu, and S. C. Wang, "High-quality factor nonpolar GaN photonic crystal nanocavities," *Appl. Phys. Lett.*, vol. 102, 191116, May 2013.

[35] M. Arita, S. Kako, S. Iwamoto, and Y. Arakawa, "Fabrication of AlGaN two-dimensional photonic crystal nanocavities by selective thermal decom-position of GaN," *Appl. Phys. Express*, vol. 5, 126502, December 2012.

[36] P. Baroni, Q. Tan, V. Paeder, and M. Roussey, "Switchable photonic crystal cavity by liquid crystal infiltration," *J. Eur. Opt. Soc.*, vol. 5, 10057, November 2010.

[37] F. Quiñónez, J. W. Menezes, L. Cescato, V. F. Rodriguez-Esquerre, H. Hernandez-Figueroa, and R. D. Mansano, "Band gap of hexagonal 2D photonic crystals with elliptical holes recorded by interference lithography," 14(11), pp. 4873-4879, May 2006.

[38] L. Vogelaar, W. Nijdam, H. A. G. M. van Wolferen, R. M. de Ridder, F. B. Segerink, E. Flück, L. Kuipers, and N. F. van Hulst, "Large area photonic crystal slabs for visible light with waveguiding defect structures: fabrication with focused ion beam assisted laser interference lithography," *Adv. Mater.*, vol. 13, no. 20, October 2001.